

Part-based Similarity Assessment between the Left and Right Retina of an Individual with Legendre Moments

Md. Iqbal Aziz Khan, Md. Rokanujjaman

(Department of Computer Science and Engineering, University of Rajshahi, Bangladesh)

Abstract: Most researches believe that the left and the right retina of an individual are different. However, in this research Legendre moments are used to show that there are some similarities between the left and right retinal images. Some parts of the whole retinal image are used in Legendre moment calculation. Most effective parts are defined and selected for Legendre moment calculation. In this approach Orthogonal Legendre moments are used for feature extraction and dimensionality reduction. Legendre moments can preserve almost all the information of the left and right retinal images in few coefficients. After extracting the Legendre features from different parts of the left and right retinal images, similarity measurement is carried out by calculating the cosine distances between the feature vectors of different parts in a left retina and the feature vectors of different parts in a right retina. Training and evaluation are performed on the publicly available datasets CHASE_DB1 and Messidor-2 respectively. The proposed method provides a high probability of finding similarities between the left and the right retinal images based on different parts.

Key Word: Legendre moments, retina, cosine similarity, biometric, part-based

Date of Submission: 27-08-2021

Date of Acceptance: 11-09-2021

I. Introduction

Some ocular diseases are associated with anatomical and functional changes in the central retinal blood vessels, the optic disc and the macula that can be observed in the retinal fundus images. Some of the anatomical changes are appeared in the retinal fundus images.

The central retinal blood vessels (CRBV) consist of the central retinal arteries and central retinal veins. The lighter colored blood is the oxygenated blood of the artery and the slightly darker blood is the deoxygenated blood of the vein. The central retinal artery branches into a superior and inferior retinal artery, each of which divides further into nasal and temporal branches. It has been shown that retinal blood vessels possess a universal unique pattern [1]. The optic disc serves as the door of entry for the central retinal artery and the door of exit for the central retinal vein. Various types of rings are observed around the optic disc margin. Usually the color of the optic disc, size and depth of the physiologic cup, cup-to-disc ratio, appearance of the rim tissue and disc borders are used for feature extraction. Larger discs have relatively more fibers than smaller discs. Smaller discs may demonstrate optic nerve head crowding [2][3]. On the other hand, the macula lutea more commonly called the macula appears as a darkened region in the central retina. The entire macula lutea can be divisible into foveola, fovea, parafoveal and perifoveal areas. It is experimentally observed that the CRBV, the optic disc and the macula is contributing individually in similarity assessment. In some works segmented CRBV is used for similarity assessment. However, performance of CRBV segmentation affects the similarity assessment. Same thing happens to the segmentation of the optic disc and the macula. Highly precise segmentation of CRBV, the optic disc and the macula is another potential research work. Therefore, part-based approach is used in this work.

If two retinas have any common anatomical feature then violation of that normalness is an indication of pathology development in the retina. As an example, the concept of asymmetry of the retinal nerve fiber layer (RNFL) may be effective for the early diagnosis of glaucoma or suspected glaucoma [4]. Moreover, the presence of unevenness between the optic nerve cup of the two eyes of an individual is considered an early sign of glaucomatous damage [5][6] clinically and is a predictor of future damage in ocular hypertensive patients [7]. Normal tolerance limits for the amount of asymmetry could be effective for early diagnosis. Once these tolerance limits are known, then patients exceeding these limits might be suspected. In case of biometric system, features found in a pairs of eyes of an individual having partial similarities could open a new door. We intend to give the researcher a new direction.

The objective of this research is to study the retinal image representing competences of Legendre moments and demonstrate their potential usefulness in the field of finding similar anatomical features between the left and right retinas of an individual using different part of the retinal images. The Legendre moments are

orthogonal and scale, translation and rotation invariants. Hence they are suitable for representing diverse features of the central retinal blood vessel, the macula and the optic disc. However, finding a best set of orders of Legendre moments for assessing the degree of similarities between different parts of the left and right retinas of an individual is very much challenging.

The rest of the paper is organized as follows. Section II is devoted to the review of the some existing approaches briefly for figuring out similarities between left and right retinas of a person. In Section III, datasets are described. Parts definition and selection is given in Section IV. Section V is presented for feature extraction using Legendre moments. Section VI is devoted to similarity measurement method. Evaluation results are presented in Section VII. Finally concluding remarks are given in the Section VIII.

II. Review of the Existing Approaches

Human volunteers based as well as algorithms based few works are found that explored similarities between anatomical features of both eyes of an individual. In [8], human volunteers were invited to comment whether a pair of the left and right retinal images displayed side-by-side belongs to the same person or two different persons. Out of 120 images they classified 95 to 99 images correctly. In another work, manual experiment was carried out to show that there is recognizable similarity in the left and right irises of an individual as well as in the irises of identical twins [9]. Manual assessment of similarities is a time consuming task that requires remarkable skills. Therefore the development of algorithms for automatic similarities measurement is of paramount importance.

Few works on finding out similarities between an individual left and right retinal image in terms of retinal blood vessels, the optic disc, macula or other features were developed based on Neural Networks (NNs). Convolutional Neural Networks (CNNs) based classifier was developed to classify the correct right retinal image up to 57% of the cases for a given left retinal image [8]. Extension of [8] is proposed in [10]. In [10], two sets of linear and nonlinear embedding were generated from the pairs of left and right retinal images and compared using the cosine similarity. The aim of [10] was to figure out which embedding can provide better cosine similarity between the left and right retinal images. However findings were the same as in [8]. Instead of measuring cosine similarity between the left and right retinal images a Y shaped neural network (YNN) was trained to find interretinal symmetry and obtained recognizable symmetry [11]. A YNN was also used in [12] and trained on a dataset of 1752 pairs of CRVs, which is much larger than the dataset used in their previous experiments, which had only 64 pairs. Moreover, classification was carried out by human volunteers and the different versions of YNN in [13]. There was a high degree of agreement between volunteers and the different YNN architectures.

In terms of fractal dimension [14], the correlation between the left and right eyes of the same person was assessed. There was no significant difference in fractal dimension between the left and right eyes.

III. Data Sets

The proposed approach is tested using an established publicly available dataset (CHASE_DB1) and evaluated quantitatively and qualitatively using a new public dataset (Messidor-2). Two pairs of sample images from two datasets are shown in Figure 1. These two public datasets have pairs of the left and right retinal images. All of these RGB datasets are converted to grayscale datasets.

CHASE_DB1 [15] contains 28 color images of the retina, captured by a Hand-held Nidek NM-200-D camera, with 999x960 pixels. It is a subset of retinal images of multi-ethnic children from the Child Heart and Health Study in England (CHASE). This dataset was collected from both left and right eyes of 14 school children.

Messidor-2 [16] contains 874 pairs of images of 874 subjects, captured by a Topcon TRC NW6 non-mydratric fundus camera with a 45 degree field of view, with 1440x960, 2240x1488 or 2304x1536 pixels and 8 bits per color channel. Each pair belongs to the left and right retina of a person. 529 pairs are taken from Messidor dataset. 345 pairs are new addition in Messidor-2 dataset.

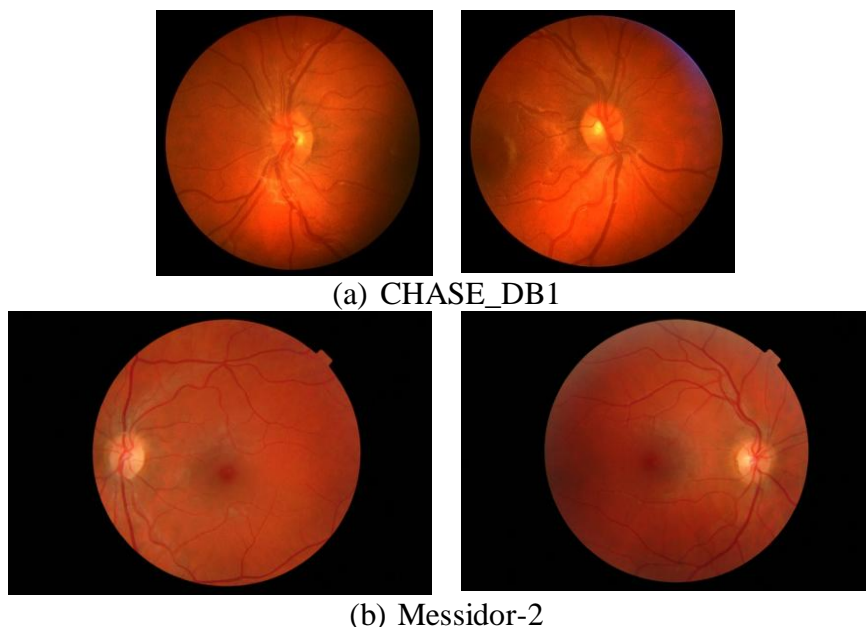


Figure 1: Two pairs of fundus images of the datasets (a) CHASE_DB1 and (b) Messidor-2

IV. Parts Definition and Selection

How to define the parts and select the most effective parts and discard the redundant parts in the left and right retinal images are described in this section. The redundant part is discarded to overcome the inter class variation and to reduce the time complexity. The retinal image is divided horizontally and vertically into different parts. However, it is observed that horizontal partitioning is more effective than vertical partitioning. The Legendre moments are calculated for different horizontal partitions. The contributions of different parts are observed in terms of Legendre moments and their cosine distance.

It should be noted that partitioning process is static. 3 to 10 parts are taken and observed their contributions. The retinal image is divided into equal parts based on their positive and negative effects. It is found that partitioning of six parts as shown in Figure 2 provide better results than other partitioning. Given six parts, different combinations of the parts are taken and used for similarity assessment. The same result is offered by several combinations based on the training dataset. The common elements in these combinations as effective are taken for our proposed similarity assessment method. In most of the cases it is noticed that uncommon elements do not have any effect on the results. Therefore, the uncommon elements are discarded from the combination. Only the remaining elements of the combination are taken for our next phase.

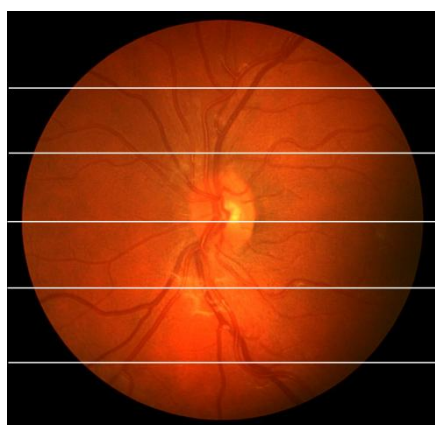


Figure 2: Six parts of a left retina

V. Legendre Moments

Legendre moments, were first introduced by Teague [17]. Legendre moments belong to the class of orthogonal moments and they are used in a lot of image processing and pattern recognition applications. The Legendre moments used Legendre polynomials as its basis set. The two-dimensional Legendre moments of order (p, q) , with an image intensity function $f(x, y)$, are defined on the square $[-1, 1] \times [-1, 1]$ as

$$L_{pq} = \lambda_{pq} \int_{-1}^1 \int_{-1}^1 P_p(x)P_q(y) f(x,y) dx dy \tag{1}$$

where $\lambda_{pq} = \frac{(2p+1)(2q+1)}{4}$, $p, q = 0, 1, 2, \dots, \infty$, and $P_p(x)$ is the p th order Legendre polynomial defined by

$$P_p(x) = \sum_{k=0}^p \left\{ \frac{(-1)^{\frac{p-k}{2}} x^k (p+k)!}{2^p k! \left(\frac{p-k}{2}\right)! \left(\frac{p+k}{2}\right)!} \right\}, \quad p-k = \text{even}$$

(Error! No text of specified style in document.)

And, the recurrent formula of Legendre polynomials is

$$\begin{cases} P_{p+1}(x) = \frac{2p+1}{p+1} x P_p(x) - \frac{p}{p+1} P_{p-1}(x) \\ P_1(x) = x, \quad P_0(x) = 1 \end{cases} \tag{3}$$

The Legendre polynomials are a complete orthogonal basis set on the interval [-1, 1]. The relation of orthogonality is defined as

$$\int_{-1}^1 P_p(x)P_q(x) dx = \frac{2}{2p+1} \delta_{pq} \tag{4}$$

where,

$$\delta_{pq} = \begin{cases} 1 & \text{if } p = q \\ 0 & \text{if } p \neq q \end{cases}$$

is the Kronecker symbol.

The orthogonal property of Legendre polynomials implies no redundancy or overlapping of information between the moments with different orders. This property enables the contribution of each moment to be unique and independent from the information in an image [17].

To compute Legendre moments from a digital image, the integrals in Equation (1) are replaced by summations and the coordinates of the image must be normalized into [-1, 1]. Therefore, the numerical approximate form of Legendre moments, for a discrete image of $M \times N$ pixels with image intensity function $f(x, y)$, is [18]

$$L_{pq} = \lambda_{pq} \sum_{i=0}^{M-1} \sum_{j=0}^{N-1} P_p(x_i)P_q(y_j) f(x_i, y_j) \tag{5}$$



where $\lambda_{pq} = \frac{(2p+1)(2q+1)}{M \times N}$, x_i and y_j denote the normalized pixel coordinates in the range of [-1, 1]. The left or right retinal images are represented by a sequence of Legendre moments L_S ,

$$\{L_0, L_1, L_2, L_3 \dots L_S\}$$

where S is the order of the moments. It is found in the experiment that the lower orders of Legendre moments mainly contain fundamental retinal image information, while the higher orders of Legendre moments preserve more detailed retinal image information. Only lower-order or only higher-order moments have few significant effects on the similarities measurement. A set of both lower-order and higher-order moments is taken from different part of the retinal images. Since in this method preprocessing algorithms such as segmentation are not used, the computational cost is drastically reduced with respect to some counterparts. Pre-processing is not performed on the images, since pre-processing is dependent on sources of images. More specifically, it is

dependent on noises, capturing devices and surrounding environments. Given Legendre moments of all the parts of the left and right retinal images of the datasets, we can easily measure their cosine similarity.

Table 1: Legendre moments for the left and right retinal images

Retina	Image	Legendre moments
Left		-2.54883216644013, -39.1841405357075, 0.519517186326675, 1.09555006610562, -0.195206187674502, -0.024244949300752, 0.001774621167093, -0.111701953187058, 0.042335373583012, 0.068560284172142, -0.019016578815481, 0.112713784523971, 0.014495142325508, 0.229014184160956, -0.016658880384136
Right		-2.44195690601696, -40.1609229725178, 0.465676337493098, 0.251467346822934, 0.2029634304591, -0.401027841891579, -0.249114685951248, 0.152025985269091, 0.120675467962824, -0.002092193401076, -0.10904412968962, 0.079295887598107, 0.063789838410484, 0.269551196825741, -0.05992901829815

VI. Cosine Distance Measurement

Given Legendre features of four parts out of six parts in the left and right retinal images of the datasets, cosine distance is measured. Two parts are discarded experimentally as less effective parts or none-effective parts. Then cosine distance is defined as

$$\cos \theta = \frac{\vec{L} \cdot \vec{R}}{\|\vec{L}\| \|\vec{R}\|} = \frac{\sum_{i=1}^n L_i R_i}{\sqrt{\sum_{i=1}^n L_i^2} \sqrt{\sum_{i=1}^n R_i^2}} \quad (6)$$

Where $\vec{L} \cdot \vec{R}$ is the dot product between the Legendre feature vector of a part in the left retinal image and a part in the right retinal image, n is the dimension of the vector. Cosine distances are calculated between four parts of a left retina and four parts of all the retinas. 16 cosine distances are found between four parts of a left retina and four parts of a right retina. Average is calculated from the 16 cosine distances for only one left-right retina pair. Similarly average is calculated for a left retina and all other right retinas in the dataset. N averages are found for a left retina and N right retinal images. All the averages are sorted and a minimum of the average values are taken for only one left-right retina pair. Similarly minimum values for other pairs are determined. Sometimes this minimum value represents the correct right retina for a given left retina. On the other hand, sometimes the actual distance between the left retina and the right retina is found in the k -th sorted average values.

VII. Results and Discussion

The performance of the proposed method for the retinal images derived from the CHASE_DB1 and Messidor-2 datasets is shown in Table 2. The performance measures are carried out only based on the value of cosine distances. Value of k is calculated from the sorted cosine distances and probability of finding a correct right retina for a given left retina is calculated based on the value of k . Smaller value of k corresponds to the lower probability of finding a right retina for a given left retina. On the other hand, larger value of k corresponds to the higher probability of having a left-right retina pair. Probability of finding a left-right retina pair in the k -nearest right retinas is shown in the Table 2. In other words for a left retinal image, its corresponding right retinal image is found in the k -nearest right retinal images with a specific probability. The two bottom rows of Table 2 show the performance of two datasets. The results of a cross-dataset experiment are shown in which our method tuned on CHASE_DB1 dataset is tested on the Messidor-2 dataset. The number of moments found optimum for CHASE_DB1 dataset is used for the Messidor-2 dataset. The number of optimum moments is not calculated for Messidor-2 dataset for impartial evaluation. Messidor-2 dataset shows probability 0.71 for $k=5$. However, CHASE_DB1 dataset reports probability 0.9 for $k=5$. The major difference in volume between the two datasets might be the one reason for different evaluation results of two datasets.

Table 2: Probability of finding similarity of left retina in k-nearest right retinas

Dataset	Values of k	Probability
CHASE_DB1	3, 5	0.78, 0.9
Messidor-2	3, 5	0.53, 0.71

VIII. Conclusion

In this paper we have shown that Legendre moment is capable enough to represent the left and right retinal images so that a high degree of similarity is found between the left and right retinal images of an individual. In this approach parts definition and selection is carried out on the retinal images. Most effective parts are taken. However, the limited range of retinal images in the CHASE_DB1 and Messidor-2 datasets do not cater for the image related characteristics such as, inter-image and intra image variability in luminance, drift in contrast and uneven background gray level values. The development of algorithms which work for the left and right retinal images captured from different imaging equipment, under different environmental conditions is also an open area for research in similarity assessment algorithms for the left and right retina.

References

- [1] C. Simon and I. Golstein, "A New Scientific Method of Identification," *New York State Journal of Medicine*, vol. 35, no. 18, pp. 901–906, 1935.
- [2] Jonas JB, Schmidt AM, Müller-Bergh JA, et al: Human optic nerve fiber count and optic disc size, *Invest Ophthalmol Vis Sci* 33(6):1992, 2012.
- [3] Quigley HA, Brown AE, Morrison JD, et al: The size and shape of the optic disc in normal human eyes, *Arch Ophthalmol* 108(1):51, 1990.
- [4] Budenz, Donald L. "Symmetry between the right and left eyes of the normal retinal nerve fiber layer measured with optical coherence tomography (an AOS thesis)." *Transactions of the American Ophthalmological Society* vol. 106 (2008): 252-75.
- [5] Fishman RS. Optic disc asymmetry. *Arch Ophthalmol* 1970;84:590-594.
- [6] I. P. Conner, J. S. Schuman, and D. L. Epstein, *Examination of the Optic Nerve*, chapter 8, pp. 81–94, Slack Incorporated, Thorofare, NJ, USA, 5 edition, 2013.
- [7] Quigley HA, Enger C, Katz J, Sommer R, Gilbert D. Risk factors for the development of glaucomatous visual field loss in ocular hypertension. *Arch Ophthalmol* 1994;112:644-649.
- [8] S. Biswas, J. Rohdin, T. Mňuk and M. Drahanský, "Is There Any Similarity Between a Person's Left and Right Retina?," 2019 International Conference of the Biometrics Special Interest Group (BIOSIG), 2019, pp. 1-8.
- [9] Hollingsworth, Karen & Bowyer, Kevin & Lagree, Stephen & Fenker, Samuel & Flynn, Patrick. (2011). Genetically Identical Irises Have Texture Similarity That Is Not Detected By Computer Vision and Image Understanding. 115. 1493-1502. 10.1016/j.cviu.2011.06.010.
- [10] S. Biswas, J. Rohdin and M. Drahansky, "Suitable Embedding to Find Similarity Between Left and Right Retinas of a Person," 2019 12th International Congress on Image and Signal Processing, BioMedical Engineering and Informatics (CISP-BMEI), 2019, pp. 1-6, doi: 10.1109/CISP-BMEI48845.2019.8965917.
- [11] S. Biswas, J. Rohdin and M. Drahansky, "Interretinal Symmetry in Color Fundus Photographs," 2020 42nd Annual International Conference of the IEEE Engineering in Medicine & Biology Society (EMBC), 2020, pp. 1980-1983, doi: 10.1109/EMBC44109.2020.9175444.
- [12] S. Biswas, J. Rohdin, and M. Drahansky, "Bilateral symmetry in central retinal blood vessels", in Proc. 8th Int. Workshop Biometrics Forensics (IWBF), Apr. 2020, pp. 1-6.
- [13] S. Biswas, J. Rohdin, A. Kavetskiy, G. Saraiva, A. Biswas and M. Drahansky, "Investigation of Bilateral Similarity in Central Retinal Blood Vessels," in *IEEE Access*, vol. 9, pp. 63012-63028, 2021, doi: 10.1109/ACCESS.2021.3074514.
- [14] V. Cosatto, "Correlation Between Right and Left Eyes in the Measurement of Retinal Vascular Fractal Dimension in an Older Population
- [15] C. G. Owen, A. R. Rudnicka, C. M. Nightingale, R. Mullen, S. A. Barman, N. Sattar, D. G. Cook, and P. H. Whincup, "Retinal arteriolar tortuosity and cardiovascular risk factors in a multi-ethnic population study of 10-year-old children; The child heart and health study in England (CHASE)," *Arterioscler Thromb Vasc Biol*, vol. 31, no. 8, pp. 1933–1938, 2011. Available at [https://staffnet.kingston.ac.uk/~ku15565/CHASE _DB1/assets/CHASEDB1.zip](https://staffnet.kingston.ac.uk/~ku15565/CHASE_DB1/assets/CHASEDB1.zip)
- [16] Etienne Decencière, Xiwei Zhang, Guy Cazuguel, Bruno Lay, Béatrice Cochener, Caroline Trone, Philippe Gain, Richard Ordonez, Pascale Massin, Ali Erginay, Béatrice Charton, Jean-Claude Klein, "Feedback on a publicly distributed database: the Messidor database." *Image Analysis & Stereology*, v. 33, n. 3, p. 231-234, aug. 2014. ISSN 1854-5165. Available at: <http://www.ias-iss.org/ojs/IAS/article/view/1155> or <http://dx.doi.org/10.5566/ias.1155>.
- [17] Teague, M.R. (1980) Image Analysis via the General Theory of Moments. *Journal of the Optical Society of America*, 70, 920-930.
- [18] K.M. Hosny. Exact Legendre moment computation for gray level images. *Pattern Recognition*, 40(12):3597-3605, 2007.

Md. Iqbal Aziz Khan. "Part-based Similarity Assessment between the Left and Right Retina of an Individual with Legendre Moments." *IOSR Journal of Computer Engineering (IOSR-JCE)*, 23(5), 2021, pp. 07-12.